A microtubule-destabilizing kinesin motor regulates spindle length and anchoring in oocytes

Jianwei Zou, Mark A. Hallen, Christine D. Yankel, and Sharyn A. Endow

Department of Cell Biology, Duke University Medical Center, Durham, NC 27710

The kinesin-13 motor, KLP10A, destabilizes microtubules at their minus ends in mitosis and binds to polymerizing plus ends in interphase, regulating spindle and microtubule dynamics. Little is known about kinesin-13 motors in meiosis. In this study, we report that KLP10A localizes to the unusual pole bodies of anastral *Drosophila melanogaster* oocyte meiosis I spindles as well as spindle fibers, centromeres, and cortical microtubules. We frequently observe the pole bodies attached to cortical microtubules, indicating that KLP10A could mediate spindle anchoring to the cortex via cortical microtubules. Oocytes treated with drugs that suppress microtubule dynamics exhibit spindles that are reoriented more vertically to the cortex than untreated controls. A dominant-negative *klp10A* mutant shows both reoriented and shorter oocyte spindles, implying that, unexpectedly, KLP10A may stabilize rather than destabilize microtubules, regulating spindle length and positioning the oocyte spindle. By altering microtubule dynamics, KLP10A could promote spindle reorientation upon oocyte activation.

Introduction

The kinesin motor proteins bind to microtubules and hydrolyze ATP to produce force and move directionally along microtubules, performing key roles in spindle assembly, chromosome attachment to the spindle, and centrosome duplication in dividing cells. The motors are also essential for integrity of the meiotic/mitotic apparatus. Remarkably, the kinesin-13 motors destabilize microtubules, linking microtubule disassembly to force production by motor proteins in the spindle (Walczak et al., 1996; Hunter and Wordeman, 2000).

The kinesin-13 motors bind to centromeres (Wordeman and Mitchison, 1995) and spindle poles (Rogers et al., 2004) and act catalytically (Hunter et al., 2003) or in the presence of the nonhydrolyzable ATP analogue, adenosine 5′-[β, γ-imido]triphosphate (Moores et al., 2002), to disassemble microtubules at the ends. They diffuse rapidly to microtubule ends but do not walk along microtubules like other kinesin motors (Helenius et al., 2006). The motors could maintain chromosome attachment to kinetochore fibers in mitosis while destabilizing the ends, driving poleward movement by coupling chromosomes to depolymerizing microtubules (Walczak et al., 1996), as well as drive poleward microtubule flux (Kwok and Kapoor, 2007). One of the two mitotic *Drosophila melanogaster* kinesin-13 motors, KLP10A, is thought to depolymerize microtubules at centromeres, and the other, KLP59C, is thought to depolymerize microtubules at spindle poles (Rogers et al., 2004), regulating spindle length (Laycock et al., 2006). KLP10A has also been reported to bind to polymerizing microtubule plus ends in interphase and modulate microtubule dynamics (Mennella et al., 2005).

The role of the kinesin-13 motors in oocyte meiosis has not been reported previously. The meiotic and mitotic divisions and their cell cycles differ in basic ways, particularly in oocytes, which typically undergo a period of arrest in meiosis I or II. The marked differences between meiosis and mitosis raise the possibility that motor regulation also differs. We report here that the kinesin-13 KLP10A localizes to anastral *Drosophila* oocyte meiotic spindles and chromosomes and, strikingly, the unusual bodies at the poles. The function of the pole bodies has not been reported previously. Our results indicate that they play an important role in anchoring the oocyte spindle to the cortex via cortical microtubules. We find evidence by analyzing a dominant-negative *klp10A* mutant that the motor unexpectedly may stabilize rather than destabilize spindle microtubules. These studies show an unusual effect of a kinesin-13 in meiosis I spindle length regulation and anchoring; it implies that regulation of spindle and cortical microtubule dynamics by KLP10A could account for spindle reorientation upon oocyte activation.

Results and discussion

To study kinesin-13 in meiosis, we designed a transgene to express full-length KLP10A fused to GFP in *Drosophila* oocytes that is

Correspondence to Sharyn A. Endow: endow@duke.edu

Abbreviations used in this paper: NCD, nonclaret disjunctional; NT, N terminus.

The online version of this article contains supplemental material.

The Journal of Cell Biology, Vol. 180, No. 3, February 11, 2008 459–466
http://www.jcb.org/cgi/doi/10.1083/jcb.200711031

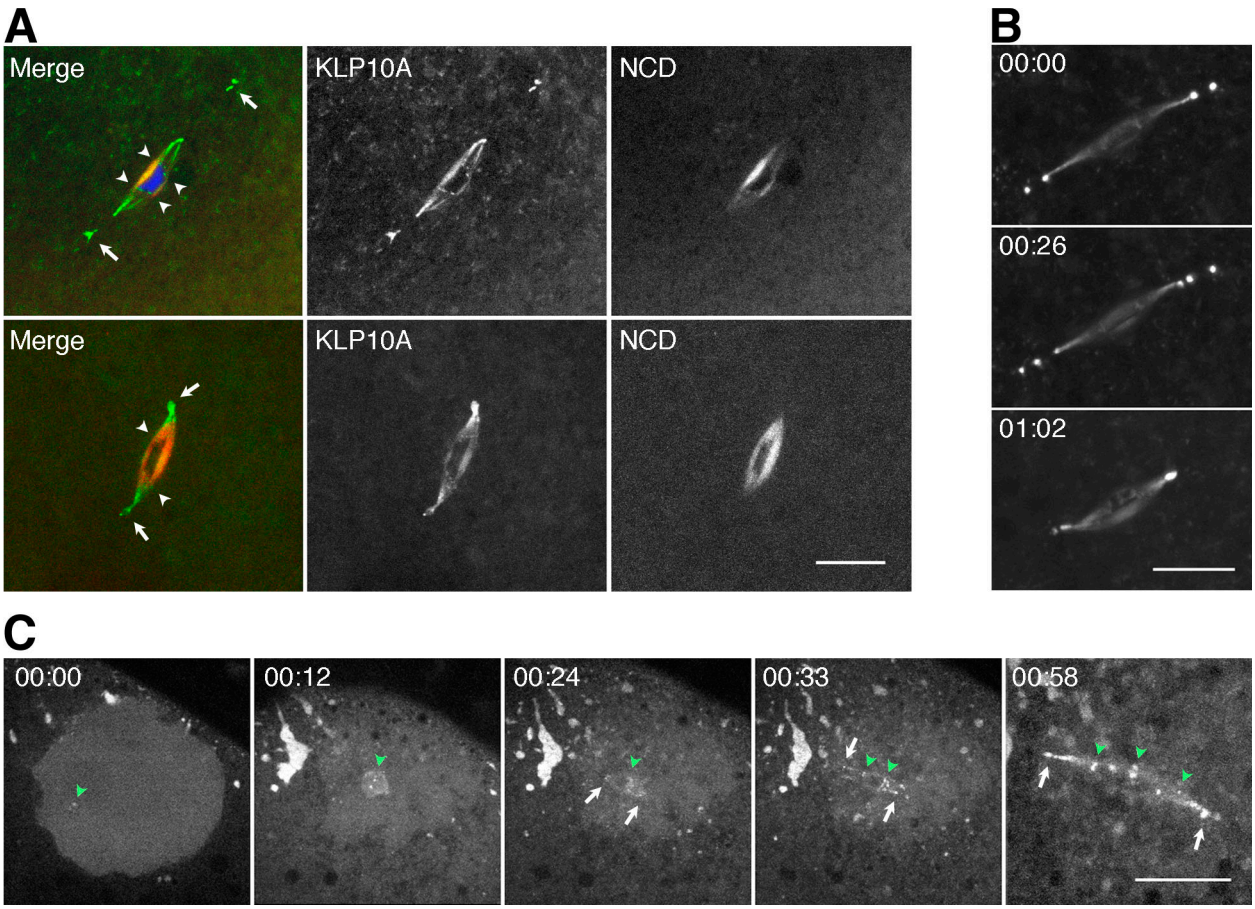

Figure 1. **KLP10A localizes to the meiosis I spindle and chromosomes.** (A) KLP10A (green) in fixed (top) or live (bottom) *klp10A-gfp/ncd–monomeric RFP* oocytes localizes to the meiosis I spindle, the unusual pole bodies (arrows), and chromosome centromeres (arrowheads). NCD (red) is present throughout the spindle but not at the pole bodies or centromeres. DNA, blue. (B) The pole bodies in live *klp10A-gfp* oocytes change in number and position over time. Time is given in hours and minutes. (C) KLP10A associates with nascent meiosis I spindle poles and centromeres early during spindle assembly. Accumulation of KLP10A around the germinal vesicle at nuclear envelope breakdown and formation of foci in the germinal vesicle (green arrowhead; left), KLP10A foci at the chromosomes (green arrowheads), poles (arrows) of the microtubule arrays that form around each bivalent chromosome during spindle assembly (center; Sköld et al., 2005), and KLP10A on the meiosis I spindle, pole bodies (arrows), and centromeres (arrowheads; right). Bars, 10 μm (C, four images at left, 20 μm).

regulated by native *klp10A* upstream sequences and recovered 10 lines representing three independent transformants. Line *M12M1* was mapped to chromosome 3, and *M6F3* was mapped to chromosome 2. Null or loss-of-function *klp10A* mutants are not available, but we tested line *M12M1* in a *klp10A*$^{+}$ genetic background for dominant-negative mutant effects on chromosome distribution in oocytes and early embryos (Komma et al., 1991). The data showed an absence of such effects (see Materials and methods).

We examined live *M12M1* oocytes using methods that we have used extensively to study meiotic spindles (Endow and Komma, 1997, 1998; Sköld et al., 2005). The oocytes showed a single bipolar spindle with a low frequency of frayed or spurred spindles (n = 2; total = 23), similar to the frequency of slightly abnormal spindles observed in wild-type *ncd-gfp* oocytes (n = 2; total = 17; Sciambi et al., 2005). The spindles were not multipolar, nor did they consist of multiple small spindles like those of mutants defective in spindle assembly (Hatsumi and Endow, 1992; Matthies et al., 1996; Sköld et al., 2005) or chromosome positioning (Theurkauf and Hawley, 1992). They assembled with the same kinetics (40.3 ± 6.3 min from the end of germinal vesicle breakdown to bipolar spindle formation; mean ± SEM; n = 4) as wild-type *ncd-gfp* oocytes (40.0 ± 1.6 min; n = 10; Sköld et al., 2005). Line *M12M1* was used for the analysis reported here.

Metaphase I spindles in fixed or live wild-type *klp10A-gfp* oocytes showed bright fluorescently labeled bodies at their poles (Fig. 1 A, arrows). Thick spindle fibers that terminated at bars or discs on the meiotic chromosomes (Fig. 1 A, arrowheads) were also fluorescently labeled and were especially prominent in fixed oocytes. At least some of these are probably kinetochore fibers interacting with kinetochores based on their bundled appearance and labeling by KLP10A of disclike structures on the chromosomes, but they could include other spindle microtubules. The most unusual of the fluorescently labeled structures were the bodies at the anastral spindle poles, which were attached to the poles or near the poles. These bodies have been observed previously (Wilson and Borisy, 1998) and were reported to contain the Msps and D-TAAC centrosomal proteins (Cullen and Ohkura, 2001) but have not previously been reported to contain microtubule motors. KLP10A binding to the meiosis I spindle, pole bodies, and meiotic chromosome centromeres was

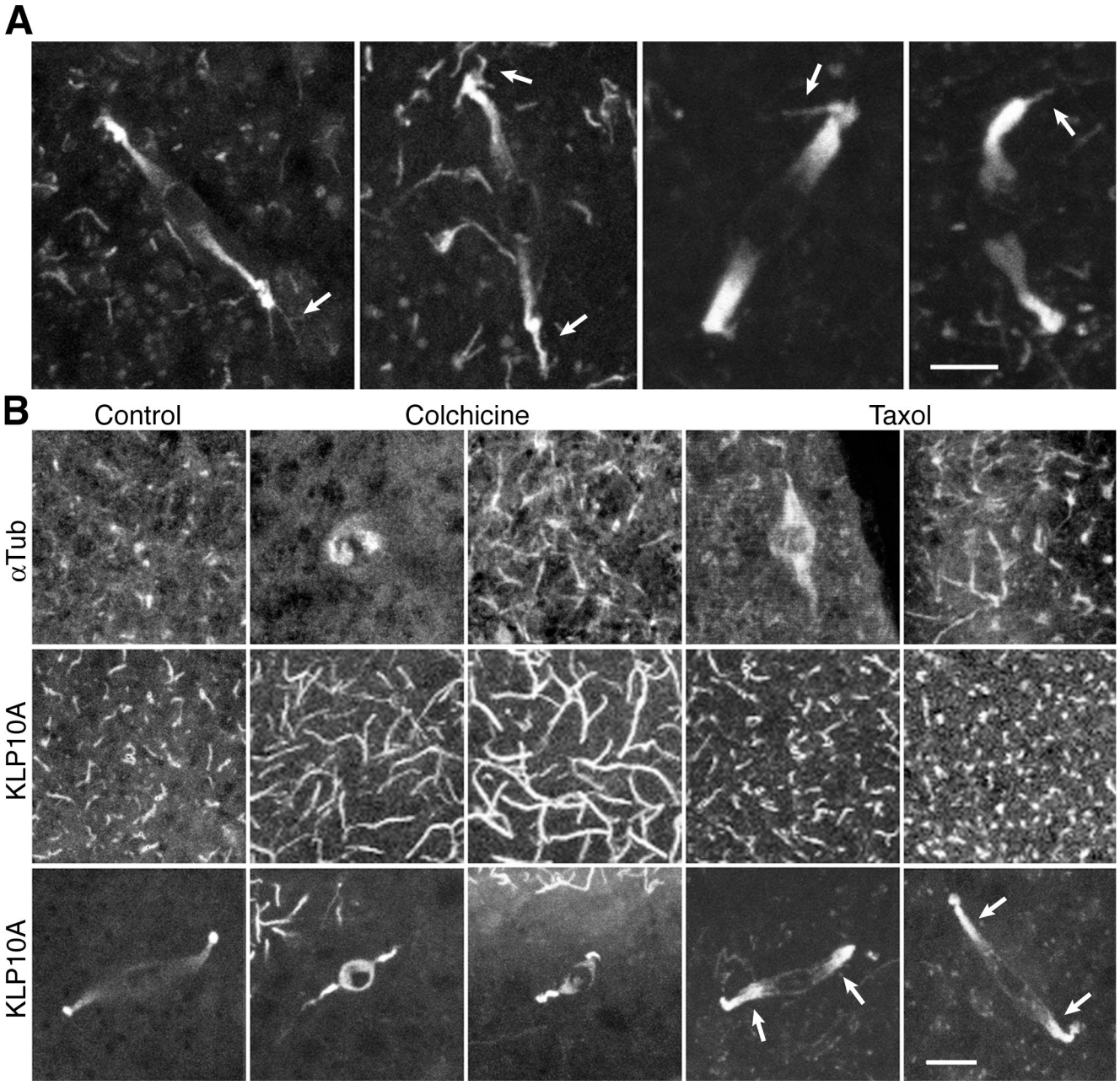

Figure 2. **KLP10A binds to both spindle poles and cortical microtubules.** (A) Meiosis I spindles in fixed *klp10A-gfp* oocytes show pole bodies attached to cortical microtubules (arrows). (B) Fixed *gfp–α-tubulin* or *klp10A-gfp* oocytes treated with microtubule-destabilizing/stabilizing drugs show changes in GFP–α-tubulin (top) or KLP10A-GFP cortical microtubule signals (middle) and spindle length (bottom). Taxol causes increased KLP10A-GFP spindle fluorescence (arrows). Bars, 5 μm (A, two images at right, 3 μm).

confirmed by staining wild-type oocytes with KLP10A antibodies (Fig. S1, available at http://www.jcb.org/cgi/content/full/jcb.200711031/DC1).

Live oocytes expressing KLP10A-GFP and the nonclaret disjunctional (NCD) kinesin-14 motor (Endow and Komma, 1997, 1998) fused to monomeric RFP (Campbell et al., 2002) showed that the two motors are distributed differently in the meiosis I spindle. Strikingly, pole body binding is observed for KLP10A but not NCD, a motor essential for oocyte spindle assembly and present on microtubules throughout the spindle (Fig. 1 A). KLP10A binds to spindle microtubules, but at low levels, and is found predominantly at spindle poles and pole bodies as well as centromeres.

The pole bodies in live, mature stage 14 oocytes were dynamic, changing in number and position with time (Fig. 1 B). Analysis of immature stage 13 oocytes showed that the pole bodies appear early during oocyte spindle assembly (Fig. 1 C). Aggregates of KLP10A are observed near the germinal vesicle at the time of nuclear envelope breakdown; KLP10A foci then form on the meiotic chromosomes and at the nascent poles of the spindlelike arrays associated with the bivalent chromosomes (Sköld et al., 2005). Assembling spindles contain several bodies at each pole that fuse to form a bipolar spindle.

Mature *klp10A-gfp* oocytes also showed fluorescent cortical microtubules near the metaphase I–arrested spindle at the

oocyte surface. Optical sections through the cortex of fixed whole-mount oocytes frequently showed microtubules attached to a pole body (Fig. 2 A, arrows). KLP10A binding to both the pole bodies and cortical microtubules implies a potential role in anchoring the meiosis I spindle to the cortex and positioning the spindle in the oocyte.

The meiosis I spindle of mature stage 14 *Drosophila* oocytes is arrested parallel to the cortex (Sonnenblick, 1950). Upon activation, the spindle rotates into a position vertical to the cortex and completes meiosis I, rapidly assembles the meiosis II spindle, and completes meiosis II (Endow and Komma, 1997, 1998). The meiosis II spindle consists of two tandem spindles (which are thought to retain the meiosis I spindle poles at the distal ends) connected by an unusual central spindle pole body (Endow and Komma, 1998). Embryos from rapidly laying *klp10A-gfp* females showed meiosis II spindles with KLP10A-labeled pole bodies at the distal ends (Fig. S2, arrows; available at http://www.jcb.org/cgi/content/full/jcb.200711031/DC1). The central spindle pole body was brightly labeled, and putative meiotic chromosome centromeres could be detected (Fig. S2, arrowheads). One pole of the meiosis II spindle was at the cortex, potentially anchoring the spindle to the cortex, whereas the other extended into the oocyte (n = 12; total = 12).

Females were fed microtubule-destabilizing/stabilizing drugs for 20–48 h to determine the effects of suppressing microtubule dynamics. Oocytes expressing GFP–α-tubulin (Grieder et al., 2000) showed long cortical microtubules after treatment with colchicine or taxol (Fig. 2 B), consistent with reports that low levels of the drugs stabilize microtubules and suppress microtubule dynamics (Derry et al., 1995; Panda et al., 1995). Oocytes of females treated with colchicine (n = 24) showed a dramatic increase in KLP10A-GFP signal length on cortical microtubules compared with untreated (n = 12) or taxol-treated oocytes (n = 24; Fig. 2 B). Colchicine is thought to inhibit microtubule polymerization and dynamics by poisoning microtubule ends upon incorporation of tubulin-colchicine, causing transient depolymerization but stabilization of surviving microtubules (Panda et al., 1995). The long KLP10A-GFP signals on cortical microtubules after colchicine treatment are unexpected and difficult to explain; they imply a structural change in the microtubule lattice that occurs upon incorporation of tubulin-colchicine at the ends, increasing KLP10A binding affinity. Alternatively, KLP10A might bind preferentially to a subset of microtubules that disassemble more readily than others, causing increased binding by the motor to those remaining.

Colchicine also resulted in highly abnormal meiosis I spindles that were much shorter (7.81 ± 0.53 μm; n = 34) than those of untreated *klp10A-gfp* females (16.1 ± 0.57 μm; n = 19; Figs. 2 B and 3 A). The spindles were deeper in the oocyte and more vertical in angle (θ = 45.6 ± 3.8°; n = 34) than untreated oocytes (θ = 8.3 ± 1.5°; n = 19; Fig. 3, A and B); spindles before activation are almost parallel to the dorsal surface. Oocytes from females treated with the microtubule-stabilizing drug, taxol, did not show an overall change in meiosis I spindle length (15.7 ± 0.64 μm; n = 38) compared with untreated oocytes. The spindle poles showed brighter KLP10A-GFP fluorescence than untreated controls (Fig. 2 B, arrows), and spindles showed small changes in depth and angle. Both were less pronounced than with colchicine (Fig. 3, A and B) and were presumably caused by the suppression of microtubule dynamics.

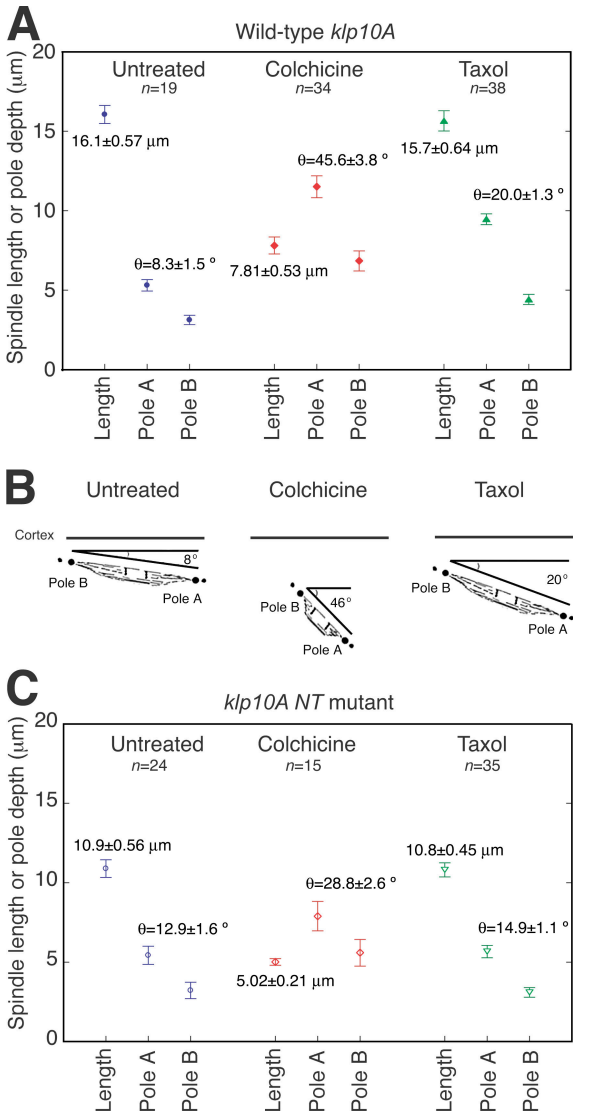

Figure 3. **Microtubule-destabilizing/stabilizing drugs affect meiosis I spindle length and orientation.** (A and C) Spindle length and pole depth from the chorion were estimated from z sections (0.5-μm steps) of fixed whole-mount *klp10A-gfp* (A) or *klp10A NT–gfp* oocytes (C) either untreated or treated with colchicine or taxol. Mean ± SEM (error bars). (B) Schematic diagram illustrating the effects of colchicine and taxol on spindle length, angle, and depth relative to the cortex in *klp10A-gfp* oocytes. Both drugs cause the spindle to move deeper into the oocyte and orient more vertically to the cortex.

Thus, microtubule drugs affect meiosis I spindle depth and angle in oocytes, indicating that spindle anchoring to the cortex involves microtubules and is dependent on microtubule dynamics. The effects of colchicine at low doses in stabilizing cortical microtubules, but causing spindles to shorten, could be the result of differences in cortical and spindle microtubule dynamics. We also observed variable effects on spindles using freshly made versus older colchicine solutions (see Materials and methods). The brighter fluorescence of spindles in taxol-treated oocytes shows that the drug affects the spindle. However, taxol did not

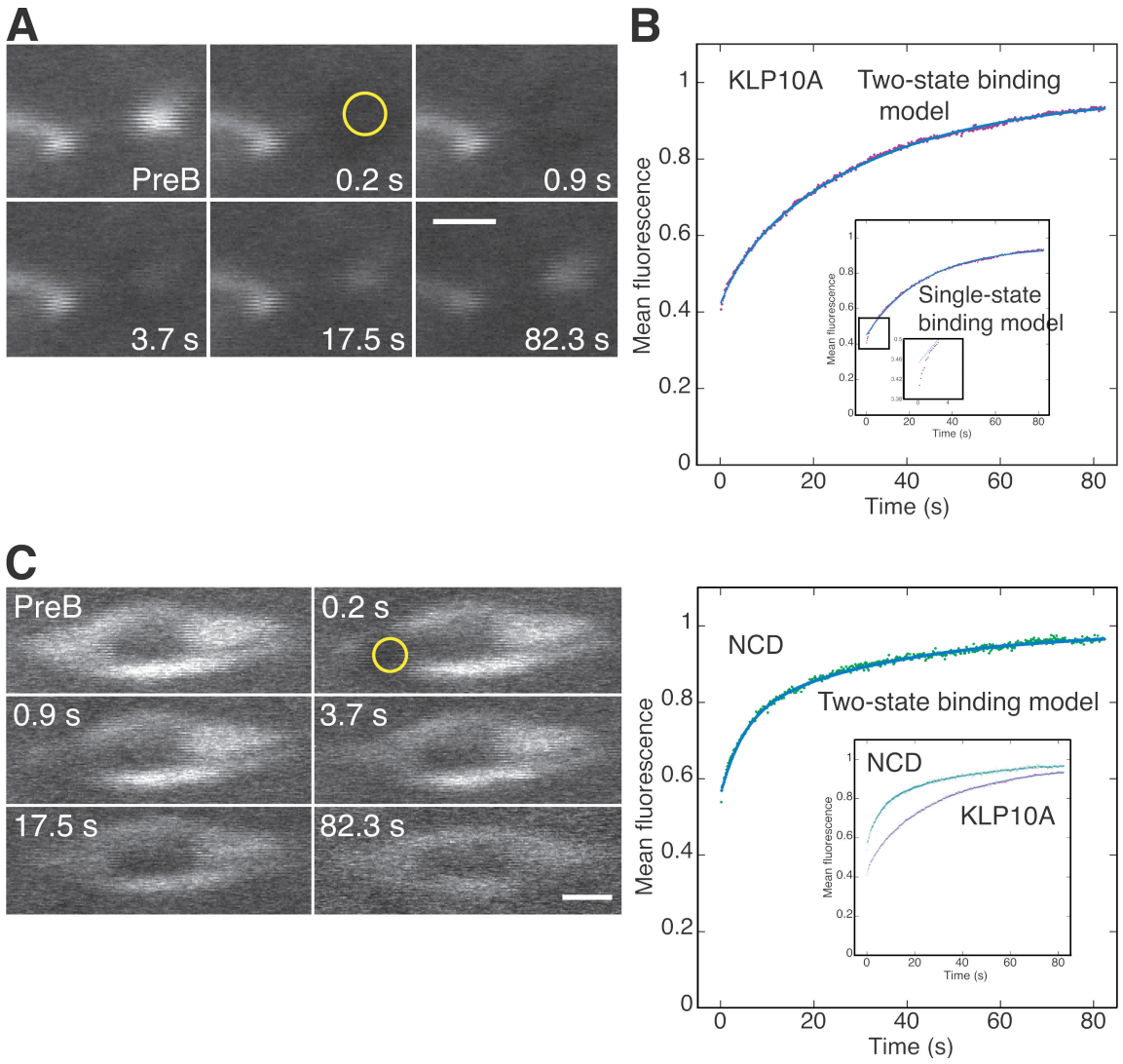

Figure 4. **FRAP analysis of KLP10A-GFP at pole bodies.** (A and C) Images from FRAP assays (Videos 1 and 2, available at http://www.jcb.org/cgi/content/full/jcb.200711031/DC1) of KLP10A-GFP at a pole body (A) and NCD-GFP in a meiosis I spindle (C) before bleaching and at exponentially increasing times during recovery. PreB, prebleach. Yellow circles indicate photobleached regions of interest (radius = 0.66 µm). (B and D) Mean fluorescence of the photobleached pole bodies (B; purple) or spindles (D; green) during recovery. Fluorescence was normalized to the first prebleach value, corrected for loss during imaging, and fit to kinetic models (blue); the two-state binding model fit well. (B, inset) Pole body data fit to the single-state binding model showed deviation at early points. (D, inset) KLP10A at pole bodies compared with NCD in spindles. Bars, 2 µm.

result in longer meiosis I spindles, as expected if KLP10A destabilizes spindle microtubules (as reported in mitosis; Rogers et al., 2004), and the drug counteracts these effects.

We also examined the effects on meiosis I spindles of a mutant, *klp10A N terminus* (*NT*), that expresses only the KLP10A NT, which targets to mitotic chromosome centromeres and spindle poles, including centrosomes, and shows a dominant-negative effect in mitosis (Maney et al., 1998; Rogers et al., 2004). Meiosis I spindles of *klp10A NT–gfp* oocytes were less brightly fluorescent than those of *klp10A-gfp* oocytes but could be easily detected and imaged. Like the full-length protein, KLP10A NT–GFP localized to meiosis I spindles, pole bodies, and centromeres but was not present on cortical microtubules. Spindles were frequently abnormal (n = 14; total = 29) with multiple or split poles and frayed spindle fibers (Fig. S3, available at http://www.jcb.org/cgi/content/full/jcb.200711031/DC1). Unexpectedly, mature meiosis I spindles of fixed *klp10A NT–gfp* oocytes were ~0.7-fold shorter in length (10.9 ± 0.56 µm; n = 24) than *klp10A-gfp* oocyte spindles (16.1 ± 0.57 µm; n = 19; Fig. 3 C) and were more vertical in angle relative to the cortex (θ = 12.9 ± 1.6°; n = 24) than wild type (θ = 8.3 ± 1.5°; n = 19).

Spindles in fixed *klp10A NT–gfp* mutant oocytes treated with colchicine or taxol were shorter by ~0.7-fold than colchichine- or taxol-treated *klp10A-gfp* oocytes (Fig. 3 C). Thus, the *klp10A NT–gfp* mutant shows dominant-negative effects in both untreated and drug-treated oocytes, consistent with the interpretation that KLP10A regulates meiosis I spindle length.

KLP10A NT presumably interferes with wild-type KLP10A function in the spindle, altering microtubule dynamics and causing spindles to shorten. If KLP10A regulates meiosis I spindle length by depolymerizing microtubules, *klp10A NT* mutant oocyte spindles should be longer than wild type; instead, the mutant

Table I. **FRAP kinetic parameters**

Motor	D_{eff}	k^*_{on}	k_{off}	$t_{1/2}$	C_{eq}	Recovery
	$\mu m^2/s$	s^{-1}	s^{-1}	s		%
KLP10A-GFP	2.3 ± 0.26					96.9 ± 0.3
Fast phase		0.037	0.201 ± 0.029	3.5	0.08 ± 0.01	
Slow phase		0.034	0.031 ± 0.0009	22	0.48 ± 0.01	
NCD-GFP	1.5 ± 0.18					98.7 ± 0.5
Fast phase		0.072	0.204 ± 0.0171	3.4	0.20 ± 0.01	
Slow phase		0.012	0.029 ± 0.0026	24	0.23 ± 0.01	

Values were obtained from curve fits of the two-state binding model (see Materials and methods) except for D_{eff} (effective diffusion coefficient), which is from fits to a diffusion-binding model (Sprague et al., 2004). C_{eq}, protein bound at equilibrium. Value ± 95% confidence interval from the curve fit.

causes spindles to shorten and detach from the cortex, indicating that KLP10A plays a role in meiosis I spindle length regulation and anchoring to the cortex. The motor could stabilize spindle fibers by cross-linking microtubules or capping microtubule ends rather than depolymerizing microtubules (Walczak et al., 1996; Hunter et al., 2003; Rogers et al., 2004; Helenius et al., 2006). Microtubule disassembly by the KLP10A motor might also be regulated (e.g., by phosphorylation), attenuating activity until after oocyte activation.

Photobleaching assays were performed to analyze KLP10A binding to the meiosis I spindle pole bodies. Data from FRAP assays of KLP10A-GFP at pole bodies were fit to kinetic models to estimate binding and dissociation constants compared with NCD-GFP in the meiosis I spindle. NCD is a spindle motor (Endow and Komma, 1997, 1998) that binds to and releases from microtubules in vitro in the presence of ATP (Chandra et al., 1993).

The assays showed slow turnover of KLP10A at pole bodies (Fig. 4 and Video 1, available at http://www.jcb.org/cgi/content/full/jcb.200711031/DC1). The data fit well to a two-state binding model (Fig. 4 B; Sprague et al., 2004); a single-state binding model (Bulinski et al., 2001; Sprague et al., 2004) also fit well, except for the early points (Fig. 4 B, inset). Both models indicated a relatively tight binding state that dominates the recovery with an early phase that is explained by the two-state binding model as a rapid, transient, much weaker binding state. At equilibrium, ∼50% of KLP10A is bound to the pole bodies in the tight-binding state and ∼10% in the weak transient state (Table I). NCD in the meiosis I spindle (Video 2) showed recovery that was poorly fit by a single-state binding model but well fit by a two-state binding model (Fig. 4). At equilibrium, ∼25% of NCD was bound in the slow, more tightly binding state, and ∼20% was bound in the transient weak state.

The kinetic parameters indicate that KLP10A binds more tightly to the pole bodies than NCD to the meiotic spindle in its slow, tight-binding state and more weakly in its transient, weak-binding state. Tight binding to the pole bodies could enable KLP10A to anchor spindles to the cortex via cortical microtubules. Transient, weak-binding diffusional interactions with microtubules are proposed to target kinesin-13 motors rapidly to microtubule ends (Helenius et al., 2006), where they bind with high affinity (Hunter et al., 2003).

Spindle length regulation, particularly in anastral oocyte spindles, is not well understood but appears to involve forces produced by microtubule sliding and disassembly/assembly and motors. We report here that suppressing microtubule dynamics significantly affects meiosis I spindle length and angle relative to the cortex. Further, a dominant-negative KLP10A mutant causes short, abnormal meiosis I spindles with frayed spindle fibers and split poles, indicating that the wild-type motor functions to regulate meiosis I spindle length and maintain spindle integrity. KLP10A could regulate microtubule dynamics in the spindle by altering the rate of switching between growth and shortening at microtubule plus ends, as for colchicine (Wilson et al., 1999). Alternatively, KLP10A could contribute to forces in the spindle, disrupting normal spindle assembly when mutant, as proposed for the kinesin-13 Kif2a (Ganem and Compton, 2004), resulting in the short spindles observed in *klp10A NT* mutant oocytes. However, low doses of colchicine might be expected to stabilize spindle microtubules, reversing these effects and restoring spindles to normal length. As neither this nor monopolar spindles like those induced by Kif2a RNAi were observed, we favor the idea that oocyte meiosis I spindles are sensitive to perturbations in microtubule dynamics caused by the KLP10A motor, resulting in changes in spindle length and integrity.

Besides spindle length, orientation of the oocyte meiotic spindle is essential to its function. The mature *Drosophila* oocyte spindle is arrested in metaphase I parallel to the dorsal surface (Theurkauf and Hawley, 1992; Endow and Komma, 1997). Our data show that the spindle is slightly tilted with one pole in or near the region of cortical microtubules. Upon oocyte activation, the spindle reorients vertical to the cortex before completing the meiosis I and II divisions (Endow and Komma, 1997, 1998). Microtubule drugs at low doses suppress cortical microtubule dynamics and phenocopy these effects by causing spindles to detach from the cortex and reorient more vertically to the surface. Spindles in the dominant-negative *klp10A NT* mutant are more vertical than wild type, indicating that KLP10A plays a role in spindle anchoring to the cortex in metaphase-arrested oocytes. Although *Caenorhabditis elegans* oocyte spindles appear to be transported to the cortex by kinesin-1 after assembly (Yang et al., 2005), *Drosophila* spindles assemble near the oocyte cortex; there is currently no information regarding spindle transport to the cortex. The stage at which KLP10A functions in spindle anchoring to the cortex is after the spindle is positioned at the cortex.

The effects of colchicine and taxol at low doses in causing spindles to detach from the cortex and reorient more vertically are paralleled by the *klp10A NT* mutant. These effects, together

with the effects of the drugs in suppressing cortical microtubule dynamics, imply that KLP10A may play a role in mediating changes that occur in the spindle upon oocyte activation by altering microtubule growth and shortening. This may be similar to the role proposed for the kinesin-13 motor, MCAK (mitotic centromere-associated kinesin), of controlling dynamic instability at microtubule plus ends in *Xenopus laevis* extract spindles (Ohi et al., 2007). Further studies will be essential to establish whether spindle reorientation in activated *Drosophila* oocytes involves microtubules and changes in dynamics mediated by the KLP10A motor.

Materials and methods

klp10A-gfp transgenes

A *CaSpeR* plasmid to express full-length KLP10A fused to S65T GFP (Heim et al., 1995), regulated by 1.685 kb of *klp10A* upstream sequences, including regions with high scores in the Reese promotor prediction tool (Reese et al., 2000), was constructed and injected into embryos to recover transgenic flies. Transgenic flies expressing a truncated KLP10A NT–GFP (M1-V274) protein regulated by the *klp10A* upstream region were similarly recovered.

Genetic tests

Genetic tests for chromosome nondisjunction and loss in oocytes and early embryos (Komma et al., 1991) were performed in a *klp10A*$^+$ genetic background to determine whether the *klp10A-gfp* transgene causes dominant-negative mutant effects. The frequency of nondisjunctional and chromosome loss offspring produced by *klp10A-gfp* females with one (n_{abn} = 4; total = 1,569; 0.25%) or two copies (n_{abn} = 6; total = 1,076; 0.56%) of the *M12M1* transgene was not significantly different from wild type (Ore R; n_{abn} = 6; total = 1,287; 0.47%). The χ^2 values correspond to P > 0.50 (1 degree of freedom), supporting the null hypothesis that the *klp10A-gfp* and wild-type females are from the same population (i.e., do not differ significantly from one another in meiotic and early mitotic chromosome segregation).

Live oocytes

Live oocytes were dissected and mounted in Schneider's *Drosophila* medium + 15% FCS as described previously (Sköld et al., 2005) to image spindle assembly in stage 13 oocytes and mature spindles in stage 14 oocytes. Under these conditions, oocytes slowly take up water from the medium, which can result in activation. Mature spindles both in live wild-type *klp10A-gfp* (13.5 ± 0.75 μm; mean ± SEM; *n* = 17) and *klp10A NT–gfp* mutant (15.0 ± 0.52 μm; *n* = 26) oocytes differed in length from fixed oocytes, most likely because of changes caused by partial activation of the oocytes during imaging.

Fixed oocytes

For fixed oocytes, ovaries of 2–4-d-old females were dissected into 170-μl fixation buffer (0.68× PBS, 0.1 M sucrose, and 5% formaldehyde, pH ∼7) to prevent activation and were teased apart. After 2.5 min, an equal volume of heptane was added, and oocytes were vortexed for 1 min. The solution was replaced with PBS, oocytes were vortexed for 30 s, and the solution was replaced again with PBS. Chorions and vitelline membranes were removed manually. Oocytes were stained with antibodies and/or DAPI and mounted in antifade under a coverslip supported by four layers of Saran wrap.

Microtubule drug treatment

1- or 2-d-old females were cultured in the dark for 20 or 40 h on *Drosophila* cornmeal-yeast-sugar-agar medium freshly mixed with 65 μg/ml colchicine. Variable effects on spindles were observed with colchicine solutions that were freshly made versus those stored at −20°C for different periods of time (5 or 16 d): the oocytes showed long cortical microtubule KLP10A signals, whereas spindles were short and abnormal after treatment with freshly made solutions, but either short or full length and normal with older solutions. This indicates that cortical microtubules are more sensitive to colchicine than spindles. Taxol-treated females were starved for 8–12 h and then placed in the dark for 20 or 48 h in a test tube containing a filter paper wick and 150 μl of 1% sucrose or glucose containing 10 μM taxol. Oocytes were fixed as above (with or without sucrose in the fixation buffer) and mounted without removing the chorion.

Microscopy

Live or fixed oocytes expressing fluorescent proteins, either GFP or GFP and monomeric RFP, were imaged at 20°C using a confocal scanhead (Radiance2100; Bio-Rad Laboratories) mounted on a microscope (Axioskop 2; Carl Zeiss, Inc.) with a 40×1.3 NA plan-NeoFluar oil immersion objective (Carl Zeiss, Inc.) and were recorded using LaserSharp 2000 software (Bio-Rad Laboratories). Z sections from the oocyte cortex through the spindle of fixed oocytes were taken in steps of 0.3–1 μm. Images of DAPI-stained chromosomes were acquired with a cooled CCD camera (PentaMAX; Princeton Instruments) attached to a microscope (Dialux 22; Leica) with a 63×1.4 NA PL APO oil immersion objective (Leica) at 22°C using IPLab Spectrum 3.1a software (Scanalytics) and were overlaid on confocal images using Photoshop CS version 8.0 (Adobe). Adjustments to image contrast and brightness were linear. Noise acquired during imaging was removed from one DNA image (Fig. S1) using the Photoshop despeckle filter.

Image analysis

Measurements of spindle depth and angle relative to the oocyte chorion were performed in NIH Image version 1.62 (National Institutes of Health). The distance, D, between spindle poles was measured from projections of the z-series images. Sections were identified in which the deeper pole A first appeared and pole B, which was closer to the surface, started to disappear. The spindle height, H, was calculated from the difference in depth of the poles, and the length, L, was calculated by $L^2 = D^2 + H^2$. The angle, θ, was calculated by θ = invsin (H/L). Spindle lengths and angles are given as the mean ± SEM.

FRAP

Photobleaching assays of KLP10A-GFP–labeled pole bodies and NCD-GFP–labeled meiosis I spindles were performed at 22–25°C using a confocal microscope (LSM510; Carl Zeiss, Inc.) and LSM 510 software (Carl Zeiss, Inc.) with a 40×1.3 NA plan-NeoFluar oil immersion objective (Carl Zeiss, Inc.) and the 488-nm line of a 30-mW Ar laser operating at 75% power. In brief, six prebleach images were recorded, and three or four photobleaching scans were performed at high laser power in a region of interest of radius *w* = 0.66 μm followed by 500 recovery images at ∼165 ms/image and low laser power (1–3%) to minimize photobleaching. The mean pixel value of the photobleached structure during recovery was recorded using LSM510 software or measured in ImageJ version 1.38x (National Institutes of Health) by manual tracking. The data were normalized to the first prebleach image and corrected for fluorescence loss during recovery by adding back the normalized fluorescence lost from an unbleached pole body or spindle region. Data from 9–17 assays were averaged and plotted versus time and then were fit to kinetic models for photobleaching recovery using Kaleidagraph version 3.6.4 (Synergy Software) or Matlab 7.4 (The Mathworks, Inc.).

The models were a single-state binding model, $y = R(1 - m2\, e^{-m1t})$, in which *y* = fluorescence, *t* = time (s), $m1 = k_{off}$, *m2* = protein bound at equilibrium (C_{eq}), and *R* = fluorescence at *t* = infinity, or a two-state binding model, $y = R(1 - m2\, e^{-m1t} - m4\, e^{-m5t})$, in which *m1* and *m2* represent k_{off} and C_{eq} for the slow state and *m5* and *m4* represent k_{off} and C_{eq} for the fast state. The remaining parameters are the same as above (Sprague et al., 2004). The recovery half-time or turnover rate, $t_{1/2} = ln2/k_{off}$, was calculated using $m1 = k_{off}$ or $m5 = k_{off}$ from the curve fits, and percent recovery was calculated as 100 × *R*. The pseudo first-order binding constant, $k^*_{on} = (m2\ m1)/(1 - m2 - m4)$ or $k^*_{on} = (m4\ m5)/(1 - m2 - m4)$ (Sprague et al., 2004), was calculated using values for *m1*, *m2*, *m4*, and *m5* from the curve fits.

The data were also fit to a diffusion-binding model, which assumes a cylinder of photobleaching and recovery by two-dimensional diffusion in the plane of focus and explains the recovery as a fast diffusional phase slowed by weak binding interactions followed by a slow, tight-binding state (Sprague et al., 2004). This model is appropriate when $k^*_{on}\, w^2/D << 1$ for the slow-binding state. We found this to be true using estimates of *D* for KLP10A-GFP of ∼7.3 μm^2/s and NCD-GFP of 6.5–16 μm^2/s, as calculated from the measured *D* for GFP, protein mass *M*, and $D \approx M^{-1/3}$ (Sprague et al., 2004) or from the Stokes' radius of dimeric full-length NCD without GFP (R_s = 7.6 nm; Tao et al., 2006) and corrected by a factor of 2–5 for the viscosity of cytoplasm (Berland et al., 1995). Fits to the model gave an effective diffusion coefficient, D_{eff}, of 2.3 ± 0.26 μm^2/s (±95% confidence interval) for KLP10A-GFP at the pole body and 1.5 ± 0.18 μm^2/s for NCD-GFP in the meiosis I spindle, which were both significantly lower than the estimated free *D* values. This indicates that diffusion during recovery is slowed by a fast binding state and/or the pole body or spindle viscosity. The two-state binding model makes no assumptions about the photobleached profile but assumes that fluorescence recovery is limited by the

kinetics of dissociation of bleached protein from the cellular structure and binding of unbleached protein. It explains the early phase of recovery as occurring by fast, weak binding instead of effective diffusion and finds kinetic parameters for this state and the slow, tight-binding state. The kinetic parameters from the two-state binding model are shown in Table I together with *D* from the diffusion-binding model.

Online supplemental material

Fig. S1 shows that KLP10A antibody staining of wild-type Ore R oocytes parallels KLP10A-GFP fluorescence, labeling the spindle, pole bodies, and centromeres. Fig. S2 shows that one pole of the meiosis II spindle, which forms from the meiosis I spindle after completion of the first meiotic division, remains at the cortex in wild-type oocytes, potentially anchoring the spindle to the cortex, and that KLP10A-GFP binds to the pole bodies, putative centromeres, and usual central spindle pole body. Fig. S3 shows that meiosis I spindles of dominant-negative *klp10A NT–gfp* mutant oocytes are frequently abnormal compared with the normal-appearing full-length *klp10A-gfp* oocyte spindles. Video 1 shows a FRAP assay of KLP10A-GFP at a pole body, and Video 2 shows a FRAP assay of NCD-GFP in a meiosis I spindle. Online supplemental material is available at http://www.jcb.org/cgi/content/full/jcb.200711031/DC1.

We thank K. Su for performing genetic tests, V. Bennett for use of the LSM510 microscope, D. Sharp for anti-KLP10A antibodies, and L. Wordeman for helpful comments.

This work was supported by grants from the National Institutes of Health and March of Dimes Birth Defects Foundation to S.A. Endow.

Submitted: 7 November 2007
Accepted: 4 January 2008

References

Berland, K.M., P.T. So, and E. Gratton. 1995. Two-photon fluorescence correlation spectroscopy: method and application to the intracellular environment. *Biophys. J.* 68:694–701.

Bulinski, J.C., D.J. Odde, B.J. Howell, T.D. Salmon, and C.M. Waterman-Storer. 2001. Rapid dynamics of the microtubule binding of ensconsin in vivo. *J. Cell Sci.* 114:3885–3897.

Campbell, R.E., O. Tour, A.E. Palmer, P.A. Steinbach, G.S. Baird, D.A. Zacharias, and R.Y. Tsien. 2002. A monomeric red fluorescent protein. *Proc. Natl. Acad. Sci. USA.* 99:7877–7882.

Chandra, R., E.D. Salmon, H.P. Erickson, A. Lockhart, and S.A. Endow. 1993. Structural and functional domains of the *Drosophila* ncd microtubule motor protein. *J. Biol. Chem.* 268:9005–9013.

Cullen, C.F., and H. Ohkura. 2001. Msps protein is localized to acentrosomal poles to ensure bipolarity of *Drosophila* meiotic spindles. *Nat. Cell Biol.* 3:637–642.

Derry, W.B., L. Wilson, and M.A. Jordan. 1995. Substoichiometric binding of taxol suppresses microtubule dynamics. *Biochemistry.* 34:2203–2211.

Endow, S.A., and D.J. Komma. 1997. Spindle dynamics during meiosis in *Drosophila* oocytes. *J. Cell Biol.* 137:1321–1336.

Endow, S.A., and D.J. Komma. 1998. Assembly and dynamics of an anastral: astral spindle: the meiosis II spindle of *Drosophila* oocytes. *J. Cell Sci.* 111:2487–2495.

Ganem, N.J., and D.A. Compton. 2004. The KinI kinesin Kif2a is required for bipolar spindle assembly through a functional relationship with MCAK. *J. Cell Biol.* 166:473–478.

Grieder, N.C., M. de Cuevas, and A.C. Spradling. 2000. The fusome organizes the microtubule network during ooctye differentiation in *Drosophila. Development.* 127:4253–4264.

Hatsumi, M., and S.A. Endow. 1992. The *Drosophila* ncd microtubule motor protein is spindle-associated in meiotic and mitotic cells. *J. Cell Sci.* 103:1013–1020.

Heim, R., A.B. Cubitt, and R.Y. Tsien. 1995. Improved green fluorescence. *Nature.* 373:663–664.

Helenius, J., G. Brouhard, Y. Kalaidzidis, S. Diez, and J. Howard. 2006. The depolymerizing kinesin MCAK uses lattice diffusion to rapidly target microtubule ends. *Nature.* 441:115–119.

Hunter, A.W., and L. Wordeman. 2000. How motor proteins influence microtubule polymerization dynamics. *J. Cell Sci.* 113:4379–4389.

Hunter, A.W., M. Caplow, D.L. Coy, W.O. Hancock, S. Diez, L. Wordeman, and J. Howard. 2003. The kinesin-related protein MCAK is a microtubule depolymerase that forms an ATP-hydrolyzing complex at microtubule ends. *Mol. Cell.* 11:445–457.

Komma, D.J., A.S. Horne, and S.A. Endow. 1991. Separation of meiotic and mitotic effects of *claret nondisjunctional* on chromosome segregation in *Drosophila. EMBO J.* 10:419–424.

Kwok, B.H., and T.M. Kapoor. 2007. Microtubule flux: drivers wanted. *Curr. Opin. Cell Biol.* 19:36–42.

Laycock, J.E., M.S. Savoian, and D.M. Glover. 2006. Antagonistic activities of Klp10A and Orbit regulate spindle length, bipolarity and function in vivo. *J. Cell Sci.* 119:2354–2361.

Maney, T., A.W. Hunter, M. Wagenbach, and L. Wordeman. 1998. Mitotic centromere-associated kinesin is important for anaphase chromosome segregation. *J. Cell Biol.* 142:787–801.

Matthies, H.J.G., H.B. McDonald, L.S.B. Goldstein, and W.E. Theurkauf. 1996. Anastral meiotic spindle morphogenesis: role of the Non-Claret Disjunctional kinesin-like protein. *J. Cell Biol.* 134:455–464.

Mennella, V., G.C. Rogers, S.L. Rogers, D.W. Buster, R.D. Vale, and D.J. Sharp. 2005. Functionally distinct kinesin-13 family members cooperate to regulate microtubule dynamics during interphase. *Nat. Cell Biol.* 7:235–245.

Moores, C.A., M. Yu, J. Guo, C. Beraud, R. Sakowicz, and R.A. Milligan. 2002. A mechanism for microtubule depolymerization by KinI kinesins. *Mol. Cell.* 9:903–909.

Ohi, R., K. Burbank, Q. Liu, and T.J. Mitchison. 2007. Nonredundant functions of kinesin-13s during meiotic spindle assembly. *Curr. Biol.* 17:953–959.

Panda, D., J.E. Daijo, M.A. Jordan, and L. Wilson. 1995. Kinetic stabilization of microtubule dynamics at steady state in vitro by substoichiometric concentrations of tubulin-colchicine complex. *Biochemistry.* 34:9921–9929.

Reese, M.G., G. Hartzell, N.L. Harris, U. Ohler, J.F. Abril, and S.E. Lewis. 2000. Genome annotation assessment in *Drosophila melanogaster. Genome Res.* 10:483–501.

Rogers, G.C., S.L. Rogers, T.A. Schwimmer, S.C. Ems-McClung, C.E. Walczak, R.D. Vale, J.M. Scholey, and D.J. Sharp. 2004. Two mitotic kinesins cooperate to drive sister chromatid separation during anaphase. *Nature.* 427:364–370.

Sciambi, C.J., D.J. Komma, H.N. Sköld, K. Hirose, and S.A. Endow. 2005. A bidirectional kinesin motor in live *Drosophila* embryos. *Traffic.* 6:1036–1046.

Sköld, H.N., D.J. Komma, and S.A. Endow. 2005. Assembly pathway of the anastral *Drosophila* meiosis I oocyte spindle. *J. Cell Sci.* 118:1745–1755.

Sonnenblick, B.P. 1950. The early embryology of *Drosophila melanogaster*. *In* Biology of *Drosophila*. M. Demerec, ed. Hafner Publishing Co., New York. pp. 62–167.

Sprague, B.L., R.L. Pego, D.A. Stavreva, and J.G. McNally. 2004. Analysis of binding reactions by fluorescence recovery after photobleaching. *Biophys. J.* 86:3473–3495.

Tao, L., A. Mogilner, G. Civelekoglu-Scholey, R. Wollman, J. Evans, H. Stahlberg, and J. Scholey. 2006. A homotetrameric Kinesin-5, KLP61F, bundles microtubules and antagonizes Ncd in motility assays. *Curr. Biol.* 16:2293–2302.

Theurkauf, W.E., and R.S. Hawley. 1992. Meiotic spindle assembly in *Drosophila* females: behavior of nonexchange chromosomes and the effects of mutations in the nod kinesin-like protein. *J. Cell Biol.* 116:1167–1180.

Walczak, C.E., T.J. Mitchison, and A. Desai. 1996. XKCM1: a *Xenopus* kinesin-related protein that regulates microtubule dynamics during mitotic spindle assembly. *Cell.* 84:37–47.

Wilson, L., D. Panda, and M.A. Jordan. 1999. Modulation of microtubule dynamics by drugs: a paradigm for the actions of cellular regulators. *Cell Struct. Funct.* 24:329–335.

Wilson, P.G., and G.G. Borisy. 1998. Maternally expressed γTub37CD in *Drosophila* is differentially required for female meiosis and embryonic mitosis. *Dev. Biol.* 199:273–290.

Wordeman, L., and T.J. Mitchison. 1995. Identification and partial characterization of mitotic centromere-associated kinesin, a kinesin-related protein that associates with centromeres during mitosis. *J. Cell Biol.* 128:95–105.

Yang, H.Y., P.E. Mains, and F.J. McNally. 2005. Kinesin-1 mediates translocation of the meiotic spindle to the oocyte cortex through KCA-1, a novel cargo adapter. *J. Cell Biol.* 169:447–457.